Design study of dedicated brain PET with polyhedron geometry

Han Shi[a,d], Dong Du[a], JianFeng Xu[b], Zhihong Su[c] and Qiyu Peng[d,*]
[a]*Tsinghua University, Beijing, China*
[b]*Huazhong University of Science and Technology, Wuhan, Hubei, China*
[c]*Southern Medical University, Guangzhou, Guangdong, China*
[d]*Lawrence Berkeley National Laboratory, Berkeley, CA, USA*

Abstract.
BACKGROUND: Despite being the conventional choice, whole body PET cameras with a 76 cm diameter ring are not the optimal means of human brain imaging.
OBJECTIVE: In fact, a dedicated brain PET with a better geometrical structure has the potential to achieve a higher sensitivity, a higher signal-to-noise ratio, and a better imaging performance.
METHODS: In this study, a polyhedron geometrical dedicated brain PET (a dodecahedron design) is compared to three other candidates via their geometrical efficiencies by calculating the Solid Angle Fractions (SAF); the three other candidates include a spherical cap design, a cylindrical design, and the conventional whole body PET.
RESULTS: The spherical cap and the dodecahedron have an identical SAF that is 58.4% higher than that of a 30 cm diameter cylinder and 5.44 times higher than that of a 76 cm diameter cylinder. The conceptual polygon-shape detectors (including pentagon and hexagon detectors based on the PMT-light-sharing scheme instead of the conventional square-shaped block detector module) are presented for the polyhedron PET design. Monte Carlo simulations are performed in order to validate the detector decoding.
CONCLUSIONS: The results show that crystals in a pentagon-shape detector can be successfully decoded by Anger Logic. The new detector designs support the polyhedron PET investigation.

Keywords: Positron emission tomography (PET), brain imaging, polyhedron geometry

1. Introduction

Clinical PET imaging is used in clinically diagnosing brain tumors and in assessing brain functional activity [1–3]. Traditionally, conventional PET cameras with 76 cm diameter ring are used for whole body tomography. Nevertheless, a dedicated brain PET offers a superior solution for human brain imaging as it has the potential to achieve better sensitivity, spatial resolution, and image quality than the 76 cm diameter PET cameras [4]. However, only cylinder or similar cylinder systems with smaller ring structure were fabricated for brain PET imaging [5–9]. Furthermore, a spherical PET (S-PET) can achieve an even higher geometrical sensitivity and a lower parallax error than conventional cylindrical ring PET scanners, thus making it a good candidate for high performance dedicated brain imaging [10–12]. However, the S-PET system has not yet been implemented because of the difficulties in designing the detector,

---

Table 1
The family of Platonic solids
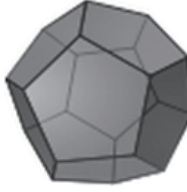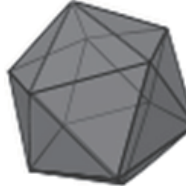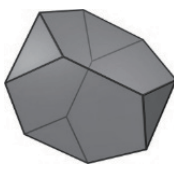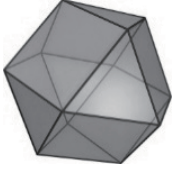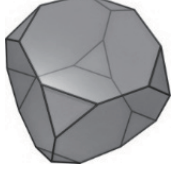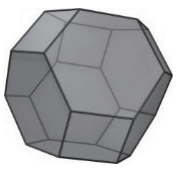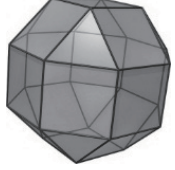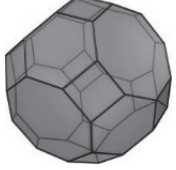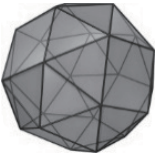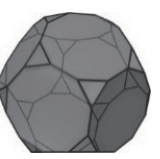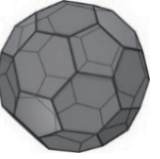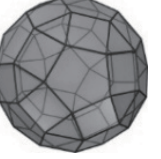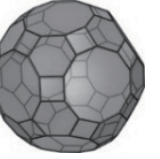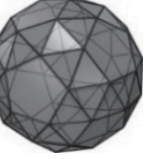
Name	Tetrahedron	Hexahedron	Octahedron	Dodecahedron	Icosahedron
Shape					
AD	0.3676	0.6366	0.5513	0.8367	0.7619

Table 2
The family of Archimedean solids

0.7017	0.7531	0.8157	0.8526	0.8727	0.9149

Note: From left to right, the polyhedrons' names are: truncated tetrahedron, cuboctahedron, truncated cube, truncated octahedron, Rhombicub-octahedron and truncated cuboctahedron.

Table 3
The family of Archimedean solids (continued)

0.8751	0.8908	0.9114	0.9409	0.9465	0.9634	0.9466

Note: From left to right, the polyhedrons' names are: snub cube, Icosido-decahedron, truncated dodecahedron, truncated icosahedron, Rhombicosi-dodecahedron, truncated icosido-decahedron and snub dodecahedron.

gantry and electronics. In contrast, convex polyhedron PETs, such as the dodecahedral PET, are easier to build and construct compared to an S-PET that requires detectors with curved surfaces, and they have the potential to achieve performances equivalent to those of S-PETs.

In this study, we first studied the geometric structure candidate including Platonic and Archimedean solids for dedicated brain PET. Then we compared the geometrical efficiency of a dodecahedron (one good case from polyhedrons) PET with three other differing candidates (an S-PET, a small cylinder PET and a conventional cylinder PET) by calculating the solid angle fractions using Monte Carlo simulation.

Based on the comparison, the advantages associated with the dodecahedron suggest it to be an optimal candidate for the geometrical structure of the dedicated brain PET. Further, the investigation of the new pentagon-shape detector module, instead of the conventional square-shaped block detector module for conventional PET [13–15], was critical for the dodecahedron brain PET. Last, we presented the conceptual pentagonal detectors based on the PMT-light-sharing scheme. Monte Carlo simulation, quite useful to PET detector design [16–18], were performed so as to investigate the new detector designs. The results show that crystals forming a pentagon-shape detector can be decoded by Anger Logic.
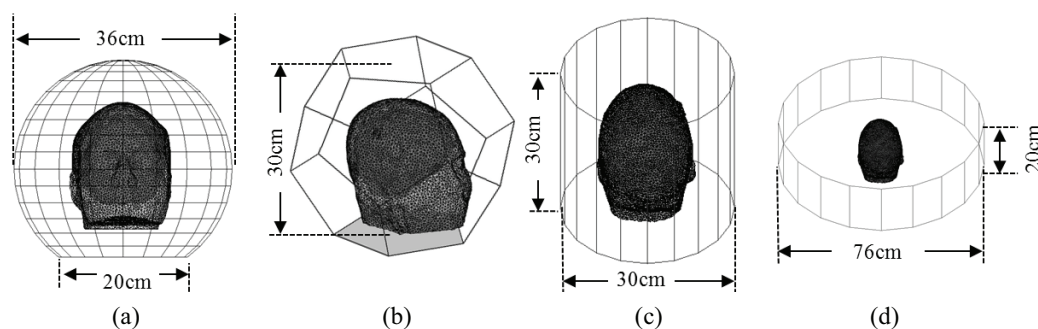
Fig. 1. Four geometries for brain PET imaging. (a) Spherical cap design; (b) Dodecahedron design; (c) Cylindrical design; (d) Conventional whole body PET.

2. Method

2.1. Polyhedron geometry structure

A spherical PET (S-PET) can potentially achieve a higher geometrical sensitivity as well as a lower parallax error than its cylindrical ring counterpart. However, designing and fabricating an S-PET that possesses curve-shaped detectors remains a challenging prospect. Convex polyhedrons consisting of flat surfaces have similar geometrical characteristics to a sphere, in terms of symmetry, solid angle coverage, and so on. In Tables 1–3 (the shape illustrations are from Wiki), the approximation degree of 18 convex polyhedrons, including 5 members from the family of Platonic solids and 13 members from the family of Archimedean solids, to the sphere are evaluated. The approximation degree (AD) is calculated as the ratio of the polyhedron surface to the circumscribed sphere surface.

2.2. Four different geometrical designs for brain PET

By taking into consideration the approximation degree, side type and number of side types, the do-decahedron was selected as the particular case of the polyhedron geometries in Section 2.1. A detailed analysis later provided in the results section (Section 3.1). Four geometrical structures are built for the dedicated brain PET as shown in Fig. 1. The first design (Fig. 1(a)) is a spherical cap ($R = 18$ cm) with an opening ($R = 10$ cm). The second design is a dodecahedron with one open face (Fig. 1(b)); the dodecahedron's inscribed sphere radius and the circumscribed sphere radius are 15 cm and 18.88 cm respectively, and the inscribed circle radius and the circumscribed circle radius of the open face are 9.28 cm and 11.47 cm respectively. Next, the third design is a cylinder with two opens in both ends (Fig. 1(c), 30 cm in both height and diameter). Finally, Fig. 1(d) shows the whole body design (20 cm in height and 76 cm in diameter). The surface areas of each of the four designs are 4019 cm^2, 3434 cm^2, 2827 cm^2, and 4775 cm^2 respectively.

2.3. Sensitivity analysis based on Monte Carlo simulation

The system sensitivity is one of the most important parameters in assessing PET cameras. Further, the system sensitivity is primarily affected by the following factors: geometrical efficiency, crystal intrinsic sensitivity, system energy, and time window settings. We assessed the geometric efficiency of each of the four systems by calculating the Solid Angle Fractions (SAF). The higher the SAF, the higher the
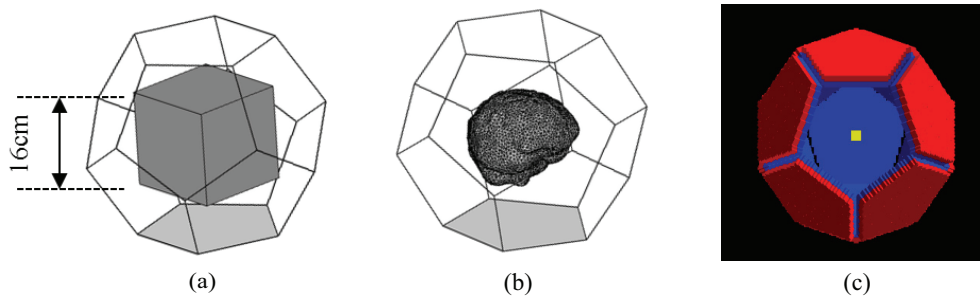
Fig. 2. Sensitivity analysis of dodecahedron PET using Monte Carlo simulation in (a) and (b) Matlab program package and (c) GATE toolkits.
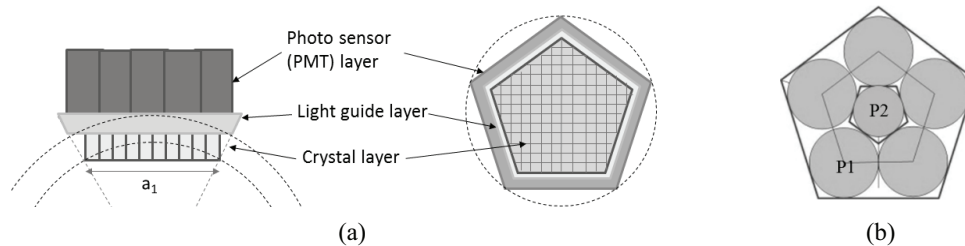

Fig. 3. Pentagon-shaped detector module design for the polyhedron PET. (a) Diagram of the detector module structure; (b) PMT assembling scheme.

geometric efficiency. The Monte Carlo simulation based on the Matlab program package was used to calculate the geometrical efficiencies of the four geometrical structures using a cubic phantom and a real brain model, as is shown in Figs 2(a) and (b). The GATE toolkit was also used to calculate the system sensitivity by considering the detector sensitivity as shown in Fig. 2(c). (Only the dodecahedron and the two cylinders are simulated, because a Spherical cap design cannot be built in GATE due to its curve face). Finally, in the GATE simulation, the crystal size is 4 mm × 4 mm × 20 mm in both the dodecahedron PET as well as the cylindrical PET.

2.4. PMT based light-sharing detector module design

For the dodecahedron PET, pentagon-shaped detector modules are required, instead of the conventional square-shaped block detector module. Figure 3 presents a conceptual pentagonal detector design that is based on the PMT-light-sharing scheme. The pentagon detector consists of a 4 mm × 4 mm × 20 mm crystals layer, a light guide layer, and the PMTs layer. l is the side length of the pentagon. Finally, the diameter ratio between P1 and P2 is 1.4259.

Monte Carlo simulations were performed to investigate the crystal decoding in a Matlab program package. To speed up the simulation, the crystal surface was set as polished so that only mirror reflections were allowed (reflection coefficient: 98.5%). Further, the crystal's attenuation length and light output were set to 1.16 cm and 26,000 ph/MeV respectively in this simulation [19]. The thicknesses of the light guides varied from 5 mm to 15 mm in the simulation. 0.2 million single events were generated in each simulation. Anger Logic is used to decode crystals for flood maps, shown as

$$\bar{x} = \frac{\sum E_i \times x_i}{\sum E_i} \quad \bar{y} = \frac{\sum E_i \times y_i}{\sum E_i}$$

Where, $\bar{x}$ and $\bar{y}$ are the two dimensional decoding positions. x_i and y_i represent the physical positions of the PMTs. E_i stands for the energy detected by the PMTs.

3. Results

3.1. Geometrical structure for polyhedron PET

The similarity or approximation degree ranges from 0 to 1. The higher the AD, the more similar the polyhedron is to the sphere. By visually examining all of the polyhedron images, it can been seen that the approximation degree is poor when the AD is less than 0.8. From among the Platonic solid family, only the dodecahedron has an AD larger than 0.8. In the Archimedean solid family, however, all of the members (except for the truncated tetrahedron and the cuboctahedron) have an AD that is larger than 0.8. In total, there are 12 polyhedrons that are good approximations of a sphere. Moreover, square-shaped detector modules are the mostly commonly used PMT-based detectors. It is feasible to build regular-polygon-shaped detector modules with 5 sides or more using conventional PMT detectors (in Section 2.4 and Section 3.3). However, building triangular detector modules using PMT does not seem to be feasible. From among the 12 polyhedrons with DAs larger than 0.8, there are five polyhedrons (the dodecahedron, truncated octahedron, truncated cuboctahedron, truncated icosahedron, and truncated icosido-decahedron) that do not have any triangle faces. Therefore, we conclude that those five polyhedrons are good candidates for geometric configurations for high performance PET systems, and more specifically, using the dodecahedron to build a PET system is more realizable because it consists of only a single type of face (the pentagon) on which detectors will be assembled. The other four polyhedrons have two or more types of face, so the dodecahedron PET was used as our preliminary study.

3.2. Geometry efficiency and system sensitivity

Figure 4 shows the volumetric illustrations of the SAFs of the four geometric structures. The spherical cap and the dodecahedron have an identical SAF that is 58.4% higher than that of the 30 cm diameter cylinder, and 5.44 times higher than that of the 76 cm diameter cylinder. SAF variances of the spherical cap and the dodecahedron are 57.4% lower than that of the 30 cm cylinder, and 45.3% lower than that of the 76 cm cylinder. Finally, based on the GATE simulation results, the system sensitivity of dodecahedron PET is 53% higher than that of the 30 cm diameter cylinder, and 5.21 times higher than that of the 76 cm diameter cylinder.

3.3. Pentagon-shape detector module decoding

For the dodecahedron PET system, the shape of the detector module is only pentagon, instead of the square shape in conventional whole body PET. Figure 5 shows the crystals decoding map of pentagon detector module with different light guide thickness. The results show the crystals can be almost decoded. The crystals located in the middle of the detector can be well decoded, but the crystals located on the edge overlap with each other. When the light guide thickness is small, the flood maps exhibit some patterns and are less uniform. In contrast, when the light guide thickness is large, the flood maps are more uniform. However, the light guide also causes some edge-effects, which then decrease the distances between the dots that are close to the edges. Therefore, the dots close to the edges become indistinguishable when the light guide is too thick.
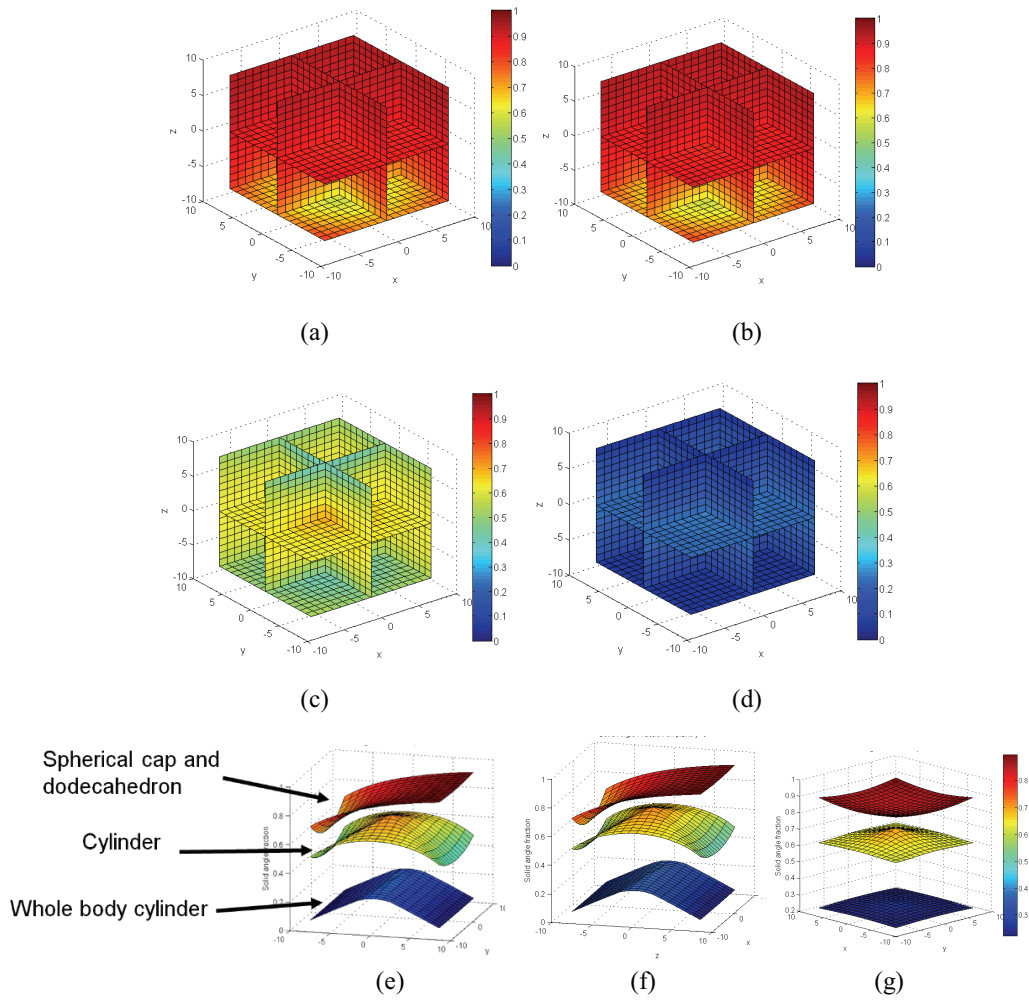
Fig. 4. Volumetric illustrations of SAF in the cubic phantom for (a) spherical cap, (b) dodecahedron, (c) cylinder and (d) whole body cylinder. Comparisons of SAFs in planes (e) $x = 0$, (f) $y = 0$ and (g) $z = 0$.
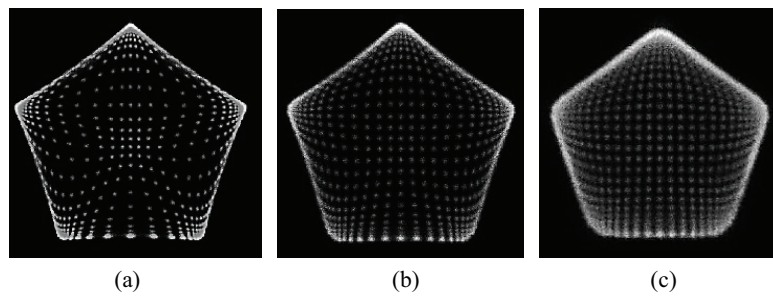

Fig. 5. (a), (b) and (c) show the flood maps of pentagonal detector with 6 PMTs. The thicknesses of the light guides are (a) 12 mm (b) 20 mm and (c) 28 mm.
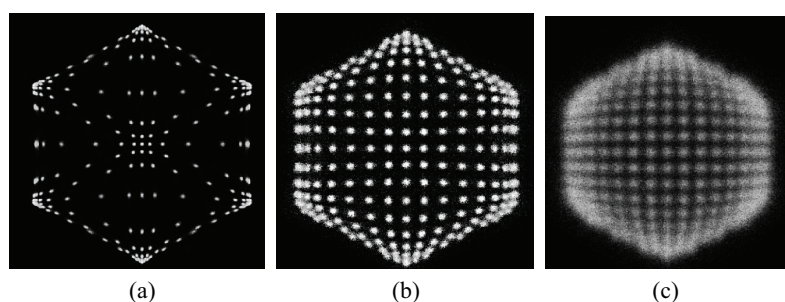
| (a) | (b) | (c) |

Fig. 6. (a), (b) and (c) show the flood maps of hexagonal detector with 7 PMTs. The thicknesses of the light guides are (a) 5 mm (b) 15 mm and (c) 25 mm.

3.4. PET geometry

The spherical cap is a better geometry for brain imaging as compared to the 30 cm or 76 cm cylinder. However, designing the detector module, gantry and read out electronics for a S-PET remains highly challenging. Further, the polyhedron is a good approximation of the spherical cap. In this study, the dodecahedron is chosen as one example of the polyhedron PET, which has the same geometrical efficiency as the spherical cap. More specifically, compared to the spherical cap, the dodecahedron is particularly advantageous: (1) It is easier to implement a dodecahedron gantry. (2) The dodecahedron PET has 11 detector sides and 1 open side. It is feasible to open and close the detector sides close to the open side in order to increase patient accessibility. (3) The 11 detector sides are identical, and there are only 46 possible coincidence combinations between the sides, which dramatically simplifies the electronics for crystal addressing and coincidence detection. Convex polyhedrons, such as the truncated octahedron, truncated cuboctahedron, truncated icosahedron, truncated icosido-decahedron, and so on, might also be suitable geometries for dedicated brain PETs.

Among the 13 excluded polyhedrons in Section 3.1, some still have special features. For example, the truncated dodecahedron consists of 12 large decagons and 20 small triangles. The triangles' surface area is only about 4.48% of the total surface area; therefore, the geometric efficiency of the system drops 4.48% if only the decagonal detector modules are installed. The extra spaces that were originally occupied by triangles could be used for other purposes, such as system calibration or monitoring. Similarly, in the Rhombicosi dodecahedron, the triangles' surface area is only about 10.83% of the total surface area.

In this preliminary study, we investigated convex polyhedral geometries that were potentially suitable for high performance PET imaging. In practice, different applications call for different requirements; this is the case for applications such as plant imaging, small animal imaging, medium/big animal imaging, human whole-body imaging, and human organ dedicated imaging. For example, one needs to consider the size of the opening for a polyhedral PET dedicated for brain imaging and, further, whether it is a possibility to open and close the detector sides that are close to the open side so as to increase patient accessibility. Therefore, prior to selecting a polyhedral geometry to implement in specific applications, the pros and cons of certain geometries should be extensively investigated. In addition to geometrical design, other issues – including the detector module design, electronics design, mechanical gantry design, system calibration methods, attenuation correction, image reconstruction algorithm, etc. – also need to be carefully studied.

3.5. Detector decoding

For the truncated icosahedron (an Archimedean solid with 12 regular pentagonal faces and 20 regular hexagonal faces, that is more similar to a sphere than a dodecahedron), both pentagon-shaped and hexagon-shaped detector modules are required. Based on our simulation, crystal decoding can be achieved not only in a pentagon detector (based on the above results), but also in other regular-polygon-shaped detectors, including hexagon-shape detector. For example, the hexagon-shape detector decoding maps are shown in Fig. 6 with different light guide thickness.

If Si-PM is used as the photodetector, the crystal decoding becomes much easier and the smaller size will reduce the detectors' volume, which also contributes to the system design.

The SAF of the dodecahedron PET is 58.4% higher than that of the 30 cm diameter cylinder, and 5.44 times higher than that of the 76 cm diameter cylinder. This demonstrates that polyhedrons with higher geometric efficiencies offer a superior replacement for the cylinder as the geometric structure of the dedicated brain PET system since they offer a higher sensitivity and signal-noise ratio. The conceptual pentagonal detectors based on the PMT-light-sharing scheme are presented for the dodecahedron PET design. Then, Monte Carlo simulations for crystal decoding show that crystals in a pentagon-shape or hexagon-shape detector can be successfully decoded by Anger Logic. Therefore, the convex polyhedron is potentially a feasible solution for high performance dedicated brain PET imaging.

Acknowledgements

References

[1] M. Villien, H. Y. Wey, J. B. Mandeville, C. Catana, J. R. Polimeni, et al. Dynamic functional imaging of brain glucose utilization using fPET-FDG. Neuroimage. 2014; 100: 192-199.

[2] E. Giovannini, P. Lazzeri, A. Milano, M. C. Gaeta and A. Ciarmiello. Clinical applications of choline PET/CT in brain tumors. Current Pharmaceutical Design. 2014; 21: 121-127.

[3] B. Suchorska, J. C. Tonn and N. L. Jansen. PET imaging for brain tumor diagnostics. Current Opinion in Neurology. 2014; 27: 683-688.

[4] K. S. M. Watanabe, T. Omura, M. Takahashi, et al. A new high-resolution PET scanner dedicated to brain research. IEEE Transactions on Nuclear Science. 2006; 49: 2557.

[5] F. Nishikido, T. Obata, et al. Feasibility of a brain-dedicated PET-MRI system using four-layer DOI detectors integrated with an RF head coil. Nucl Instrum Meth A. 2014; 756: 6-13.

[6] P. Rato Mendes, J. Alberdi, M. Canadas, et al. Design and prototyping of a human brain PET scanner based on monolithic scintillators. 2010 IEEE NSS/MIC Record. 2010: 2798-2800.

[7] J. Seguinot, A. Braem, E. Chesi, C. Joram, S. Mathot, et al. Novel geometrical concept of a high-performance brain PET scanner. Principle, design and performance. Nuovo Cimento Della Societa Italiana Di Fisica C-Colloquia on Physics. 2006; 29: 429-463.

[8] K. Soonseok, W. Wai-Hoi, L. Hongdi, et al. High resolution GSO block detectors using PMT-quadrant-sharing design for human whole body and breast/brain PET applications. IEEE NSS/MIC Record. 2006: 2863-2867.

[9] M. Schmand, K. Wienhard, M. E. Casey, et al. Performance evaluation of a new LSO high resolution research tomograph – HRRT. 1999 IEEE NSS/MIC Record. 1999: 1067-1071.

[10] C. B. L. J. B. Ra, Z. H. Cho, S. K. Hila and J. Correll. A true three-dimensional reconstruction algorithm for the spherical positron emission tomograph. Phys. Med. Biol. 1982; 27: 37-51.

[11] K. S. H. Z. H. Cho and S. K. Hilal. Spherical positron emission tomograph (S-PET)I - performance analysis. Nucl Instrum Meth A, 1984; 225: 422-438.

[12] N. M. Moghaddam, A. Karimian, S. M. Mostajaboddavati, et al. Preliminary design and simulation of a spherical brain PET system (SBPET) with liquid xenon as scintillator. Nukleonika. 2009; 54: 33-38.

[13] E. V. Roncali and S. R. Cherry. Design considerations for DOI-encoding PET detectors using phosphor-coated crystals. IEEE Transactions on Nuclear Science. 2014; 61: 67-73.

[14] S. T. Liu, S. H. An, H. D. Li, et al. A dual-layer TOF-DOI detector block for whole-body PET. IEEE Transactions on Nuclear Science. 2012; 59: 1805-1808.

[15] Y. Yongfeng, W. Yibao, Q. Jinyi, S. S. James, et al. A prototype PET scanner with DOI-encoding detectors. Journal of Nuclear Medicine. 2008; 49: 1132-40.

[16] G. Santin, D. Strul, D. Lazaro, et al. GATE: A Geant4-based simulation platform for PET and SPECT integrating movement and time management. IEEE Transactions on Nuclear Science. 2003; 50: 1516-1521.

[17] M. Janecek and W. W. Moses. Simulating scintillator light collection using measured optical reflectance. IEEE Transactions on Nuclear Science. 2010; 57: 964-970.

[18] D. J. van der Laan, D. R. Schaart, M. C. Maas, et al. Optical simulation of monolithic scintillator detectors using GATE/GEANT4. Physics in Medicine and Biology. 2010; 55: 1659-1675.

[19] H. Peng, P. D. Olcott, et al. Investigation of a clinical PET detector module design that employs large-area avalanche photodetectors. Physics in Medicine and Biology. 2011; 56: 3603-3627.